Crystal and Molecular Structure of Trichloro-oxobis(triphenylphosphine oxide)tungsten(v), (1). Single-crystal Electron Spin Resonance Spectra of (1) and Tetraphenylarsonium Aquatetrachloro-oxotungstate(v) and Electronic Structures of these and Some Related Molybdenum(v) Compounds

By **Lesley H. Hill, Nepal C. Howlader,** and **Frank E. Mabbs,*** Department of Chemistry, University of Manchester, Manchester M13 9PL
Michael B. Hursthouse and **K. M. Abdul Malik,** Department of Chemistry, Queen Mary College, Mile End Road, London E1 4NS

The crystal structure of (1) has been determined by *X*-ray crystallographic methods. The compound crystallises in the monoclinic space group $C2/c$ with a = 14.002(6), b = 13.059(7), c = 19.158(8) Å, β = 96.00(3)°, and Z = 4. The $[WOCl_3(PPh_3O)_2]$ molecule is disordered over two orientations in the crystal and possesses a crystallographically imposed C_2 axis passing through the W atom. The disordered atoms are Cl(2) and O(2). Molecular dimensions are W–Cl(1), 2.369(4); W–O(1), 2.088(11); W–Cl(2), 2.242(10); and W–O(2), 2.053(22) Å. Single-crystal e.s.r. spectra of (1) diluted in the niobium analogue gave g_1 = 1.739 ± 0.002, g_2 = 1.763 ± 0.002, and g_3 = 1.770 ± 0.002, whilst a similar study on $[AsPh_4][WOCl_4(OH_2)]$ gave $g_{\parallel}$ = 1.806 ± 0.001 and $g_{\perp}$ = 1.765 ± 0.001. The e.s.r. data for $[WOCl_3(PPh_3O)_2]$, $[MoOCl_3(PPh_3O)_2]$, and $[MoOCl_3\{P(NMe_2)_3O\}_2]$ are discussed in terms of an angular-overlap model for their electronic structures.

THE occurrence of molybdenum in a number of redox enzyme systems has prompted a great deal of activity in the study of the chemistry of this element. Some of our recent work on the reactivity and electronic structures of molybdenum(v) complexes have provided evidence for possible mechanisms by which molybdenum may act, in for example nitrate reductase.[1-8] It has been reported [9] that plants grown with tungsten instead of molybdenum form the tungsten analogue of nitrate reductase, but there is no nitrate reductase activity (only the dehydrogenase activity). In view of this we feel that it is of interest to compare the reactivities and electronic structures of similar complexes of molybdenum and tungsten, in order to provide information on any differences in the chemistry of what are often regarded as chemically very similar elements. As part of this study we now report a single-crystal structural and e.s.r. study of $[WOCl_3(PPh_3O)_2]$ along with a comparison of similar properties of $[AsPh_4][WOCl_4(OH_2)]$, $[MoOCl_3(PPh_3O)_2]$, and $[MoOCl_3\{P(NMe_2)_3O\}_2]$.

EXPERIMENTAL

Syntheses.—*Trichloro-oxobis(triphenylphosphine oxide)-tungsten*(v). Mixing solutions of tungsten pentachloride (1.8 g) and triphenylphosphine oxide (2.8 g) in dried methyl cyanide gave an immediate bluish green precipitate. Recrystallisation from dry methyl cyanide gave crystals suitable for *X*-ray crystallographic and single-crystal e.s.r. studies (Found: C, 50.4; H, 3.6; Cl, 12.3; P, 6.9; W, 21.3. Calc. for $C_{36}H_{30}Cl_3O_3P_2W$: C, 50.1; H, 3.5; Cl, 12.3; P, 7.2; W, 21.3%).

Tetraphenylarsonium aquatetrachloro-oxotungstate(v). This was obtained as small pale blue crystals by the addition of a solution of tetraphenylarsonium chloride in a minimum volume of methanol to a solution of tungsten pentachloride in concentrated hydrochloric acid. Attempts to grow larger crystals for single-crystal electronic absorption spectroscopy have been unsuccessful (Found: C, 39.3; H, 3.0; Cl, 18.5; W, 24.7. Calc. for $C_{24}H_{22}AsCl_4O_2W$: C, 38.8; H, 3.0; Cl, 19.1; W, 24.8%). *X*-Ray powder photography showed that this compound is isomorphous with the molybdenum analogue.[6]

Crystal Data.—$C_{36}H_{30}Cl_3O_3P_2W$, M = 862.8, Monoclinic, a = 14.002(6), b = 13.059(7), c = 19.158(8) Å, β = 96.00(3)°, U = 3 483.9 Å^3, space group $C2/c$ (C_{2h}^6 No.15), D_m = 1.51 g cm^{-3} (flotation), Z = 4, D_c = 1.527 g cm^{-3}, $F(000)$ = 1 620, μ(Mo-K_α) = 32.6 cm^{-1}, λ(Mo-K_α) = 0.710 69 Å.

The crystal used for intensity measurements had overall dimensions 0.45 × 0.30 × 0.20 mm, and was bounded by the six intersecting planes [($\bar{1}$ 1 1), (1 $\bar{1}$ $\bar{1}$), (0 0 1), (0 0 $\bar{1}$), (1 1 $\bar{1}$), ($\bar{1}$ $\bar{1}$ $\bar{1}$)]. The preliminary unit-cell parameters and crystal system were determined from oscillation and Weissenberg photographs. Accurate lattice parameters were determined from least-squares refinement of the setting angles for 25 reflections automatically centred on a Nonius CAD4 diffractometer. The systematic absences, h k l for $h + k$ odd and $h0l$ for l odd, suggested the space groups $C2/c$ (No. 15) or Cc (No. 9), the former being confirmed by subsequent structure analysis. The intensities of 3 423 reflections ($1.5 < \theta < 25°$) were recorded using monochromatised Mo-K_α radiation and an ω—2θ scan technique. Two standard intensities monitored at intervals of 1 h did not show any significant variation during data collection. The intensities were corrected for Lorentz, polarisation, and absorption effects. Equivalent reflections were averaged and those with $I_0 < 2\sigma(I_0)$ were omitted to obtain a total of 2 705 unique reflections.

Structure Analysis and Refinement.—The structure was solved and refined on the basis of space group $C2/c$. With Z = 4, only one half of the molecule constitutes an asymmetric unit and the W atom is required to lie on a special position. A three-dimensional Patterson map was interpreted to obtain the position of the W atom (0.00, 0.129, 0.25) on a two-fold axis. This interpretation required that the molecule must be disordered in some way. Least-squares refinement of the W atom parameters (R = 0.32) was followed by a difference electron-density synthesis from which the W–O–P linkage and one Cl atom [Cl(1)] were

obtained. Further refinement and difference syntheses revealed the positions of the phenyl C atoms. The difference map also contained a peak *ca.* 10 e Å^{-3} in height at *ca.* 2.0 Å from the W position. This peak was considered to represent disordered Cl [Cl(2)] and O [O(2)] atoms, and one position was included in the refinement with a contribution of 0.5 from each atom. With anisotropic temperature factors for all non-hydrogen atoms except Cl(2) and O(2), the R value fell to 0.14. A difference map at this stage showed clearly that the disordered Cl and O atoms in fact occupied *two* positions separated by *ca.* 0.7 Å. When these two positions were refined for Cl(2) and O(2), the R value dropped to 0.085. Attempts to refine the structure with W(1)–Cl(2) and W(1)–O(2) distances fixed at 2.375 and 1.667 Å respectively, did not improve the R value and the isotropic temperature factors for Cl(2) and O(2) showed marked increases. It was therefore concluded that the 'free' Cl(2) and O(2) positions give the best fit for the observed diffraction data. Attempts to refine the structure in the space group Cc, where all atoms may occupy general positions, resulted in unacceptable bond lengths and angles. So the refinement was continued on the disordered model in space group $C2/c$. The positions of the H atoms on the phenyl ring were calculated (C–H = 1.08 Å) and their contributions included in the calculation of F_c. One common U_{iso} was included in the refinement for all H atoms and had a final value of 0.14(2) Å^2. The weighting

TABLE 1

Final non-hydrogen atomic fractional co-ordinates (× 10^4)

Atom	x	y	z
W(1)	0 *	1 261(1)	2 500 *
Cl(1)	1 608(3)	1 452(3)	3 005(3)
P(1)	206(3)	3 203(3)	1 248(2)
Cl(2)	448(7)	−24(8)	1 829(5)
O(2)	−324(17)	413(20)	3 346(12)
O(1)	320(8)	2 452(9)	1 835(6)
C(11)	−477(10)	2 700(13)	477(9)
C(12)	−360(14)	1 697(15)	286(10)
C(13)	−848(20)	1 323(19)	−324(14)
C(14)	−1 464(14)	1 970(23)	−739(13)
C(15)	−1 572(13)	2 902(20)	−555(12)
C(16)	−1 116(13)	3 300(15)	46(11)
C(21)	1 382(11)	3 504(12)	996(11)
C(22)	2 115(13)	3 558(13)	1 555(14)
C(23)	3 033(14)	3 845(15)	1 413(13)
C(24)	3 165(13)	4 094(17)	716(13)
C(25)	2 435(17)	4 027(18)	168(15)
C(26)	1 522(16)	3 773(16)	308(15)
C(31)	−347(11)	4 353(14)	1 504(9)
C(32)	−1 274(13)	4 273(16)	1 730(11)
C(33)	−1 772(14)	5 115(16)	1 864(12)
C(34)	−1 341(20)	6 048(18)	1 824(17)
C(35)	−431(24)	6 097(17)	1 598(20)
C(36)	71(14)	5 319(13)	1 454(10)

* Parameters held invariant due to space-group symmetry.

scheme applied was $w = 1/[\sigma^2(F_o) + 0.000\,3\,F_o^2]$, and this gave satisfactory analyses of variance. The refinement finally converged at $R = 0.083$ and $R' = 0.086$. Neutral-atom scattering factors were taken from ref. 10 (for W), ref. 11 (for Cl, P, O, and C), and ref. 12 (for H), with those for the heavier atoms being modified for anomalous dispersion.[13] All crystallographic computations were performed on the Queen Mary College ICL 1904 S and University of London CDC7600 computers with programs SHELX [14] for structure solutions and refinement and PLUTO [15] for drawing molecular diagrams.

Electron Spin Resonance Spectra.—E.s.r. spectra were recorded as previously described [16] on single crystals of $[WOCl_3(PPh_3O)_2]$, and tungsten-diluted $[NbOCl_3(PPh_3O)_2]$ at room temperature and 150 K, and on $[AsPh_4][WOCl_4(OH_2)]$ at room temperature. The crystals were mounted (using standard X-ray techniques) such that the magnetic field could be oriented in the ab, bc^*, and ac^* crystallographic planes for the monoclinic system, and in a plane containing

TABLE 2

Intramolecular interatomic distances (Å) and interbond angles (°)

(*a*) Co-ordination polyhedron

W(1)–Cl(1)	2.369(4)	W(1)–Cl(2)	2.242(10)
W(1)–O(1)	2.088(11)	W(1)–O(2)	2.053(22)
Cl(1)–W(1)–Cl(1′) *	167.9(3)	Cl(2)–W(1)–O(2)	98.5(8)
Cl(1)–W(1)–Cl(2)	90.1(3)	Cl(2)–W(1)–O(2′)	17.4(9)
Cl(1)–W(1)–Cl(2′)	99.0(3)	Cl(2)–W(1)–O(1)	96.7(5)
Cl(1)–W(1)–O(2)	90.8(7)	Cl(2)–W(1)–O(1′)	175.9(8)
Cl(1)–W(1)–O(2′)	95.7(8)	O(2)–W(1)–O(2′)	114.7(14)
Cl(1)–W(1)–O(1)	85.1(3)	O(2)–W(1)–O(1)	164.3(8)
Cl(1)–W(1)–O(1′)	85.9(5)	O(2)–W(1)–O(1′)	80.9(8)
		O(1)–W(1)–O(1′) *	83.7(7)
Cl(2)–W(1)–Cl(2′)	83.1(5)		

(*b*) PPh_3O Ligand

		C(21)–C(22)	1.406(26)
		C(22)–C(23)	1.392(27)
P(1)–O(1)	1.488(12)	C(23)–C(24)	1.406(32)
P(1)–C(11)	1.799(17)	C(24)–C(25)	1.389(34)
P(1)–C(21)	1.808(16)	C(25)–C(26)	1.374(30)
P(1)–C(31)	1.782(20)	C(21)–C(26)	1.398(33)
C(11)–C(12)	1.375(24)	C(31)–C(32)	1.415(22)
C(12)–C(13)	1.380(29)	C(32)–C(33)	1.340(25)
C(13)–C(14)	1.395(33)	C(33)–C(34)	1.365(29)
C(14)–C(15)	1.280(32)	C(34)–C(35)	1.390(40)
C(15)–C(16)	1.360(28)	C(35)–C(36)	1.282(33)
C(11)–C(16)	1.393(22)	C(31)–C(36)	1.398(24)
W(1)–O(1)–P(1)	159.9(7)	C(12)–C(11)–C(16)	117.8(1.7)
O(1)–P(1)–C(11)	112.7(7)	C(11)–C(12)–C(13)	120.0(1.9)
O(1)–P(1)–C(21)	108.5(7)	C(12)–C(13)–C(14)	119.3(2.3)
O(1)–P(1)–C(31)	111.3(8)	C(13)–C(14)–C(15)	120.2(2.3)
C(11)–P(1)–C(21)	106.3(9)	C(14)–C(15)–C(16)	122.5(2.1)
C(11)–P(1)–C(31)	108.9(8)	C(11)–C(16)–C(15)	120.1(2.0)
C(21)–P(1)–C(31)	108.9(8)	C(22)–C(21)–C(26)	122.9(1.8)
P(1)–C(11)–C(12)	119.9(1.2)	C(21)–C(22)–C(23)	118.7(2.3)
P(1)–C(11)–C(16)	122.4(1.5)	C(22)–C(23)–C(24)	117.6(2.1)
P(1)–C(21)–C(22)	114.9(1.6)	C(23)–C(24)–C(25)	123.0(1.8)
P(1)–C(21)–C(26)	121.9(1.5)	C(24)–C(25)–C(26)	119.5(2.5)
P(1)–C(31)–C(32)	117.4(1.5)	C(21)–C(26)–C(25)	118.0(2.4)
P(1)–C(31)–C(36)	123.0(1.3)		
		C(32)–C(31)–C(36)	119.5(1.8)
		C(31)–C(32)–C(33)	120.7(1.9)
		C(32)–C(33)–C(34)	118.7(2.0)
		C(33)–C(34)–C(35)	118.9(2.3)
		C(34)–C(35)–C(36)	124.8(2.2)
		C(31)–C(36)–C(35)	117.2(2.0)

* The primed atom is generated by symmetry, $-x, y, \frac{1}{2}-z$, and belongs to one and the same molecule.

the parallel and perpendicular molecular orientations in the tetragonal crystals.

Electronic Spectral Measurements.—Since we have been unable to grow crystals sufficiently large for single-crystal polarised absorption spectra we only report the spectra of poly(dimethylsiloxane) mulls of the two compounds. These were recorded in the range 6 000—30 000 cm^{-1} as described previously.[17]

RESULTS AND DISCUSSION

Crystal Structure.—The fractional co-ordinates of the non-hydrogen atoms are given in Table 1 and the derived interatomic distances and interbond angles in Table 2. The hydrogen-atom parameters, the anisotropic temperature factors for the heavier atoms, and lists of

observed and calculated structure factors have been deposited in Supplementary Publication No. SUP 22781 (15 pp.).*

The crystal structure (Figure 1) consists of discrete molecules of $[WOCl_3(PPh_3O)_2]$ held together by Van der Waals' forces. The structure of a single molecule is

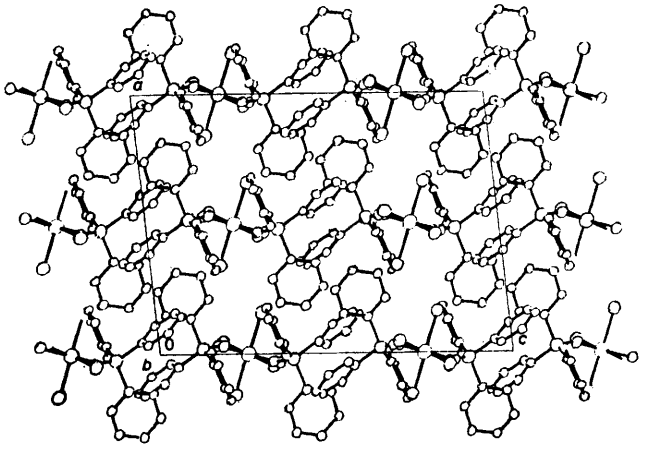

FIGURE 1 Molecular packing in $[WOCl_3(PPh_3O)_2]$ viewed along *b*

shown in Figure 2, which also indicates the atom-numbering scheme used. The molecule is disordered over two orientations in the crystal, and possesses a crystallographically imposed C_2 axis passing through the W atom. The metal atom has a distorted octahedral geometry with two mutually *cis* PPh_3O groups and two mutually *trans* Cl atoms; the remaining two co-ordination sites are occupied by the disordered Cl and O(oxo) atoms

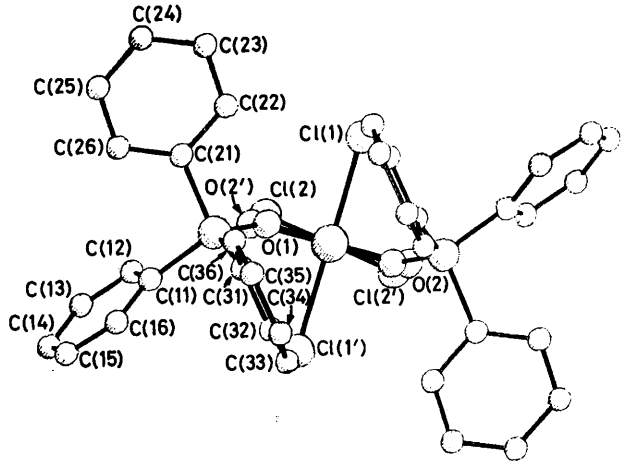

FIGURE 2 The structure of a single molecule of $[WOCl_3(PPh_3O)_2]$ and the atom-numbering system in the asymmetric unit. Viewed down *b* (C_2 axis)

[Cl(2) and O(2)]. Similar metal co-ordination has also been observed in the related complexes $[WSCl_3(PPh_3O)_2]$,[18] $[MoOCl_3(PPh_3O)_2]$,[8] and $[MoOCl_3\{P(NMe_2)_3O\}_2]$.[7] The present complex is essentially isostructural with the sulphido-derivative, the only difference being that in the latter the disordered S and Cl atoms occupy only one site each side of the C_2 axis, whereas in the present complex the different W–Cl and W=O distances result in separate identification of the two 'half-atoms'. The W–O(PPh_3O) distance (2.09 Å) is comparable with the corresponding distances in $[WSCl_3(PPh_3O)_2]$ (2.06 Å) and in the molybdenum compounds mentioned above (2.06—2.14 Å).[7,8] The W–Cl bond length (2.369 Å) and Cl–W–Cl angle (167.9°) involving the mutually *trans* Cl atoms are identical with the sulphido-analogue, but the W–Cl distance for the disordered Cl atom is slightly longer (2.24 *vs.* 2.20 Å).

With reference to W–O(2) representing the terminal W–O(oxo) direction, a comparison of corresponding bond angles with those in both the ordered and disordered molecules of $[MoOCl_3(PPh_3O)_2]$ [8] indicates that the tungsten complex is more angularly distorted. In particular the O(2)–W–O(1')–P angle is less than 90°. This is an unusual feature compared with monomeric six-co-ordinate molybdenum(v) oxo species, where the

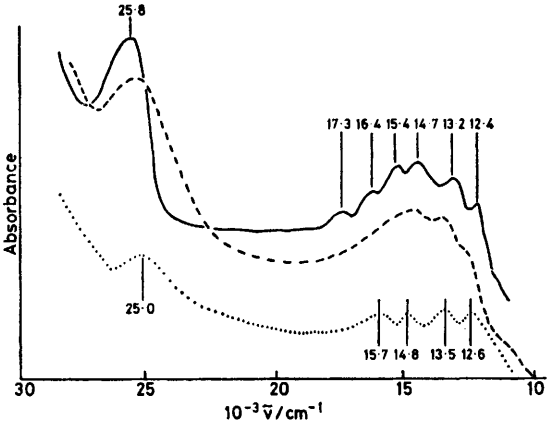

FIGURE 3 Electronic absorption spectra of mulls of $[WOCl_3(PPh_3O)_2]$ at 5 K (· · ·), $[AsPh_4][WOCl_4(OH_2)]$ at 295 K (– – –), and $[AsPh_4][WOCl_4(OH_2)]$ at 5 K (——)

angles between the terminal oxo-group and the *cis* ligands are usually greater than 90°.

The geometry of the PPh_3O ligand shows no unusual features and has dimensions: P–O = 1.49, P–C = 1.80 (mean), and C–C = 1.37 Å (mean); O–P–C = 109—113, C–P–C = 106—109, P–C–C = 117—123, and C–C–C = 117—123°. The W–O–P angle is 159°.

Electronic Absorption Spectra.—$[AsPh_4][WOCl_4(OH_2)]$. The electronic absorption spectrum of a mull of this compound in the range 10 000—30 000 cm^{-1}, at both room temperature and 5 K, consisted of two band envelopes, see Figure 3. The lower-energy band envelope is partially resolved at both temperatures. This fine structure can be interpreted in terms of two electronic origins at 12.4 and 14.7 × 10^3 cm^{-1}, upon which are superimposed progressions of *ca.* 850 cm^{-1}. This band system, by analogy with the corresponding molybdenum system, is assigned to the excitation $b_2^*(5d_{xy}, W\text{–}Cl\pi^*) \rightarrow e^*(5d_{xz,yz}, W\text{–}O\pi^*)$. In this case the separation of 2 300 cm^{-1} between the two electronic origins

* For details see Notices to Authors No. 7, *J.C.S. Dalton*, 1979, Index issue.

represents the value of the spin–orbit coupling constant in the complex. The progressions involving quanta of *ca.* 850 cm^{-1} correspond to ν(W=O) in the excited state. This frequency is reduced from that in the ground state (980 cm^{-1}) as expected for such an electronic excitation. The second band envelope centred on *ca.* 25.5 × 10^3 cm^{-1} shows no structure. We assume that the assignment of this band is analogous to that of the molybdenum system, which could be either $b_2^*(5d_{xy}, W{-}Cl\pi^*) \rightarrow b_1^*(5d_{x^2-y^2}, W{-}Cl\sigma^*)$ or $e(5d_{xz,yz}, W{-}O\pi) \rightarrow b_2^*(5d_{xy}, W{-}Cl\sigma^*)$. Although we have recently advanced arguments in favour of the latter in the molybdenum systems, the interpretation of the spectra is not unambiguous.

$[WOCl_3(PPh_3O)_2]$. The electronic absorption spectrum of a mull of this compound is very similar to that of $[AsPh_4][WOCl_4(OH_2)]$, see Figure 3, and we assume that apart from the change in symmetry the assignments are the same. The low-energy band envelope can be interpreted in terms of two electronic origins (12.6 and 14.8 × 10^3 cm^{-1}) each with at least one vibrational component of *ca.* 900 cm^{-1} corresponding to W=O in the excited state. In this case the two electronic origins represent the components of the $e^*(d_{xz}, d_{yz})$ level split by a combination of the low-symmetry ligand field and spin–orbit coupling. If we assume ξ_w to be 2 300 cm^{-1}, as estimated for $[WOCl_4(OH_2)]^-$, then the energies of the two components of the doublet due to the ligand-field splitting alone are at 13.4 and 13.9 × 10^3 cm^{-1} respectively in a first-order approximation.

Electron Spin Resonance Spectra.—$[AsPh_4][WOCl_4(OH_2)]$. This compound is isomorphous with the molybdenum analogue, and the crystals belong to a tetragonal space group. The single-crystal e.s.r. spectrum at room temperature did not show any tungsten hyperfine structure. Least-squares fitting of the angular variation of the e.s.r. spectrum gave $g_{\parallel} = 1.806 \pm 0.001$ and $g_{\perp} = 1.765 \pm 0.001$, where $g_{\parallel}$ coincide with the terminal W=O direction.

$[WOCl_3(PPh_3O)_2]$. Single-crystal e.s.r. measurements of undiluted crystals at both room temperature and 150 K showed only one signal at all orientations in each of the *ab*, *bc**, and *ac** crystallographic planes; the data are in Table 3. These observations indicate that there are significant magnetic interactions between the molecules in the unit cell; *cf.* for example $[MoOCl_3\{P(NMe_2)_3O\}_2]$.[7] In order to overcome the difficulties inherent in finding the molecular *g* values under such circumstances we have obtained the e.s.r. spectra for single crystals of $[NbOCl_3(PPh_3O)_2]$ containing 1—2% tungsten. $[NbOCl_3(PPh_3O)_2]$ has been shown to be isomorphous with the tungsten analogue.[18] At room temperature the e.s.r. spectra were broad and resembled those of the undiluted system. However, cooling the crystals to 150 K enabled the inequivalent molecules to be identified, but only in the *ab* crystallographic plane. These data are in Table 3. Treatment of the data according to the method of Schonland [19] resulted in the principal molecular *g* values and their direction cosines with respect to the crystallographic axes given in Table 4.

TABLE 3

Angular variation of the e.s.r. spectrum of pure $[WOCl_3(PPh_3O)_2]$ at room temperature and tungsten-diluted $[NbOCl_3(PPh_3O)_2]$ at 150 K (ν = 34.940 GHz)

	$[WOCl_3(PPh_3O)_2]$			Tungsten-diluted $[NbOCl_3(PPh_3O)_2]$			
	Resonance field *H*/G †			Resonance field *H*/G			
				ab plane, *a* at θ = 0			
θ/°	*ab* plane *a* at θ = 0	*bc** plane *b* at θ = 0	*ac** plane *a* at θ = 0	Molecule 1	Molecule 2	*bc** plane *b* at θ = 0	*ac** plane *a* at θ = 0
0	14 226	14 161	14 226	14 203	14 203	14 147	14 205
15	14 221	14 171	14 283			14 156	14 264
30	14 210	14 197	14 349	14 155	14 212	14 172	14 317
45	14 193	14 234	14 385	14 138	14 204	14 195	14 355
60	14 177	14 273	14 396	14 131	14 180	14 220	14 360
75	14 164	14 296	14 357	14 137	14 169	14 253	14 332
90	14 160	14 305	14 306	14 147	14 147	14 272	14 270
105	14 164	14 295	14 241	14 169	14 137	14 253	14 211
120	14 177	14 271	14 184	14 194	14 133	14 220	14 158
135	14 193	14 234	14 152	14 210	14 145	14 195	14 130
150	14 210	14 196	14 146	14 214	14 163	14 172	14 130
165	14 221	14 170	14 182			14 156	14 156
180	14 226	14 161	14 226	14 203	14 203	14 147	14 205

† 1 G = 10^{-4} T.

In order to facilitate the interpretation of the e.s.r. data we have defined a molecular axis system as: *z* parallel to W–O(2) (which we take to be the terminal oxo-group), *y* perpendicular to *z* and in the W–O(2)–Cl(2) plane, and *x* perpendicular to this plane. The relationship between the principal molecular *g* values and this molecular axis system is given in Table 5. As in low-symmetry oxomolybdenum(V) systems that we have reported,[7,8,20] none of the principal molecular *g* values coincides with the metal–oxo direction, or with any other particular metal–ligand directions. The reason for the tilting of the principal *g* values from the molecular axis system is the small but very important off-diagonal elements in the molecular *g* tensor, see Table 6. The non-zero off-diagonal tensor elements may be attributed to metal *d*-orbital mixing caused by the low-symmetry

ligand field. The values of the mixing coefficients cannot be obtained algebraically from the experimental data and any particular theoretical model, because of the complicated nature of the equations involved. We have attempted to overcome this difficulty by calculating the electronic structure of the system using the angular-overlap method. The use of this method however does involve the assumption that only electronic states involving metal based *d*-orbital functions are important in determining the e.s.r. and electronic absorption spectra of the systems.

Angular Overlap Calculation.—The approach has been to use the known molecular geometry with respect to a chosen axis system and to treat the angular-overlap parameters e_σ, $e_{\pi x}$, and $e_{\pi y}$ for each ligand as empirically adjustable parameters. In this way the *d*-orbital energies and their associated wave functions can readily be calculated, as outlined by Gerloch and Slade.[21] Using these *d*-orbital functions and energies, the molecular *g* tensor was calculated using the perturbation method of Abragam and Pryce.[22] Diagonalisation of the *g* tensor then gave the principal molecular *g* values and their orientations with respect to the chosen axis system. The squares of these principal *g* values were then transformed into the crystallographic *a*, *b*, *c** axis system and the angular variation of the e.s.r. spectrum was calculated for comparison with the experimental data. The method of approach has been to vary the angular-overlap parameters to fit as many features of the absorption spectra as possible, and finally to vary the orbital-reduction parameters k_x, k_y, k_z and the metal spin–orbit coupling constant, ξ_M, until the best fit to the principal molecular *g* values and angular variation of the e.s.r. spectrum was obtained. This approach has been applied to $[WOCl_3(PPh_3O)_2]$, and to $[MoOCl_3(PPh_3O)_2]$ and $[MoOCl_3\{P(NMe_2)_3O\}_2]$ which have geometries similar to that of the tungsten compound.

$[WOCl_3(PPh_3O)_2]$. Using the geometry derived from the *X*-ray crystal structure it is possible to find a combination of angular-overlap parameters which will predict electronic transitions to within 1 000 cm^{-1} of those observed. The set of energy levels and associated wave functions enable the molecular *g* tensor to be calculated.

TABLE 4

Principal molecular *g* values and their direction cosines with respect to the crystallographic axes for tunsten-diluted $[NbOCl_3(PPh_3O)_2]$ at 150 K

	Direction cosines					
	Alternative 1			Alternative 2		
g values	*a*	*b*	*c**	*a*	*b*	*c**
g_1 1.739	−0.602 5	0.076 2	0.794 5	0.601 8	−0.110 4	0.791 0
g_2 1.763	0.403 1	−0.830 1	0.385 3	−0.364 7	0.843 2	0.395 1
g_3 1.770	−0.688 9	−0.552 4	−0.469 4	0.710 5	0.526 2	−0.467 2

The estimated errors on the *g* values are ±0.002.

TABLE 5

Angles between principal molecular *g* values and the chosen *x*, *y*, and *z* axes for tungsten-diluted $[NbOCl_3(PPh_3O)_2]$

Molecular direction †	Direction cosines		
	a	*b*	*c**
x	−0.904 9	−0.094 7	−0.414 9
y	0.298 1	−0.836 6	−0.459 4
z	−0.303 6	−0.539 5	0.785 3

	Angle					
	Alternative 1			Alternative 2		
Molecular value	*x*	*y*	*z*	*x*	*y*	*z*
g_1	78.0	127.5	40.0	149.6	95.3	60.1
g_2	116.5	50.4	51.1	85.1	174.6	91.9
g_3	29.5	61.8	82.0	119.9	90.8	150.1

† See text for the definition of the molecular axis system.

For a fixed ξ_w a suitable choice of *k* values allows the calculation of g_{ii} almost identical to the experimentally derived values in Table 6. For a given ξ_w and energy levels the choice of *k* values which reproduce correctly the g_{ii} values is restricted, since k_i almost entirely determines the value of g_{ii}. However, the calculation gave

TABLE 6

Molecular *g* tensors derived from the experimental principal molecular *g* values and the chosen molecular *x*, *y*, and *z* axis system

Alternative 1			Alternative 2		
x	*y*	*z*	*x*	*y*	*z*
1.767 1	0.006 6	−0.002 6	1 746 4	0.001 1	0.012 2
0.006 6	1.756 1	0.011 4	0.001 1	1.762 6	−0.000 3
−0.002 6	0.011 4	1.750 0	0.012 2	−0.000 3	1 764 2

values of g_{ij} which are larger in magnitude than the experimental values. The consequence of this is that the calculated principal molecular *g* values are incorrect. Particularly we find the smallest and largest calculated values fall outside the range of the experimental values. A consequence of this is that the calculated angular variation of the e.s.r. spectrum is in very poor agreement with experiment. Other combinations of angular-overlap parameters which correctly predict the absorption spectrum do not improve the situation.

One objection to the calculation described above is that it predicts the transition $d_{xy}^* \rightarrow d^*_{x^2-y^2}$ at *ca.* 25 × 10^{-3} cm^{-1}. Our previous discussions concerning the energy of this transition in the oxomolybdenum(v) systems suggested that it should be at much higher energy.[7] On this basis we have increased the value of e_σ for the ligands *cis* to the oxo-group. This increases the d_{xy}^*–$d^*_{x^2-y^2}$ energy separation. The calculation of the *g* values now requires a larger value of k_z. However, this device does

not improve the e.s.r. calculation. Indeed, the values of g_{ij} are even larger in magnitude, and consequently the agreement with the principal molecular g values and the angular variation of the e.s.r. spectrum is worse.

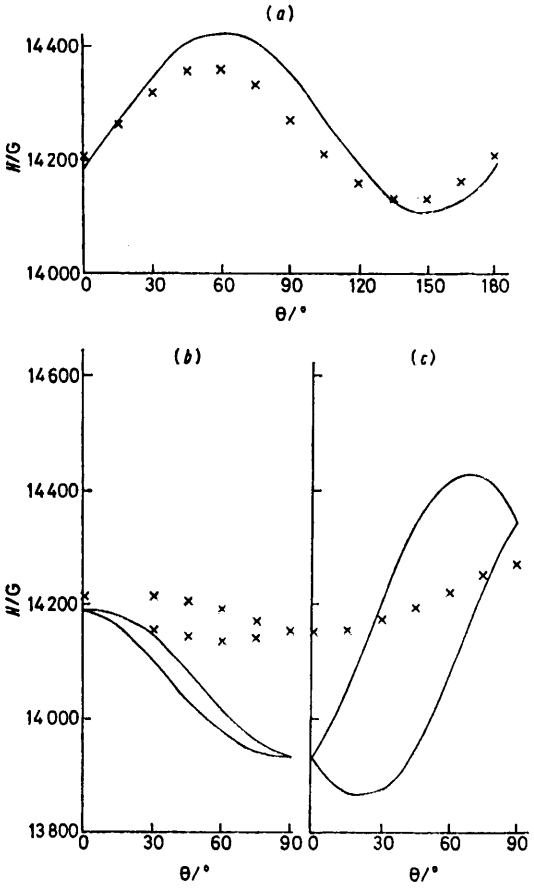

(d)

Relative d-orbital energies/10^3 cm^{-1}	Wave functions
62.8	$-0.9949d_{z^2}$ $-0.0979d_{yz}$ $-0.0199d_{xz}$ $-0.0038d_{xy}$ $+0.0098d_{x^2-y^2}$
23.9	$0.0178d_{z^2}$ $-0.2745d_{yz}$ $-0.0114d_{xz}$ $-0.0013d_{xy}$ $-0.9614d_{x^2-y^2}$
14.1	$-0.0975d_{z^2}$ $+0.8915d_{yz}$ $+0.3574d_{xz}$ $+0.0066d_{xy}$ $-0.2606d_{x^2-y^2}$
13.1	$-0.0164d_{z^2}$ $+0.3466d_{yz}$ $-0.9336d_{xz}$ $+0.0161d_{xy}$ $-0.0882d_{x^2-y^2}$
0.0	$0.0029d_{z^2}$ $+0.0122d_{yz}$ $-0.0126d_{xz}$ $-0.9998d_{xy}$ $-0.0019d_{x^2-y^2}$

FIGURE 4 Comparison of the experimental (×) and calculated (——) e.s.r. data for tungsten-diluted $[NbOCl_3(PPh_3O)_2]$ at 150 K: (*a*) *ac**, (*b*) *ab*, (*c*) *bc** crystallographic planes, and (*d*) relative *d*-orbital energies and the associated wavefunctions. The calculation was for θ = 93.5° for Cl(1) and Cl(1′), θ = 96.1° for Cl(2), and θ = 83.3° for Cl(1); e_σ (oxo) = 52.0 × 10^3, e_π (oxo) = 16.0 × 10^3, e_σ (L_{cis}) = 10.5 × 10^3, e_π (L_{cis}) = 2.0 × 10^3, e_σ (L_{trans}) = 10.0 × 10^3, e_π (L_{trans}) = 1.0 × 10^3 cm^{-1}, k_x = 0.86, k_y = 0.93, k_z = 0.56, and ξ_w = 2 100 cm^{-1}

The reason why the calculation over estimates g_{ij} could be the use of a geometry which is too distorted. In order to test this we have performed the calculation using θ = 93.5° for Cl(1) and Cl(1′), θ = 83.3° for O(1′)–P, and θ = 96.1 for Cl(2). These latter two values represent the limits of the θ values when the standard deviations are considered. The results of such a calculation are in Figure 4 (in Figures 4—6 orbitals with coefficients $<10^{-3}$ have been omitted). This represents an improvement in fitting the e.s.r. data, but the argeement is still very poor.

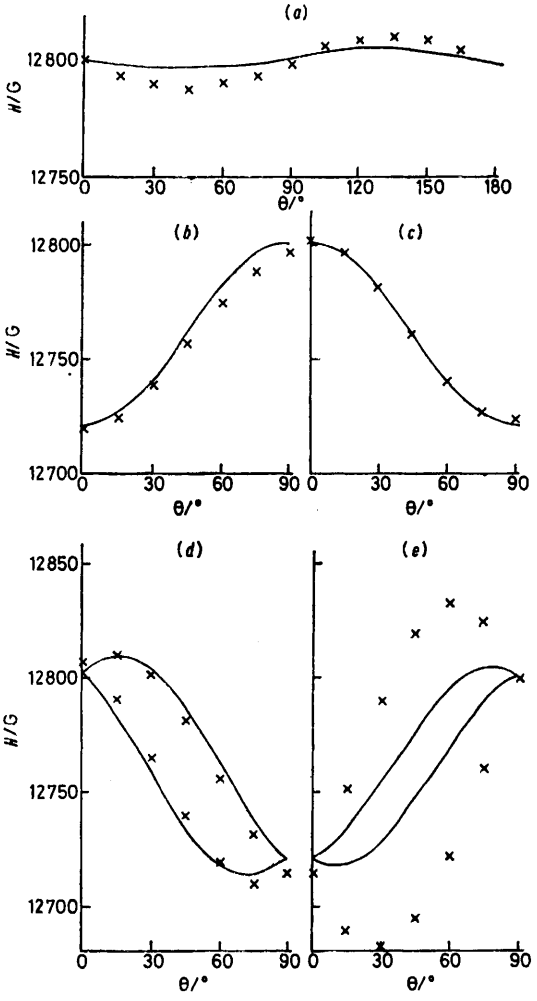

(f)

Relative d-orbital energies/10^3 cm^{-1}	Wave functions
59.3	$0.9976d_{z^2}$ $-0.0144d_{yz}$ $-0.0022d_{xz}$ $-0.0030d_{xy}$ $+0.0671d_{x^2-y^2}$
22.8	$0.0672d_{z^2}$ $+0.0198d_{yz}$ $-0.0512d_{xz}$ $+0.0416d_{xy}$ $-0.9954d_{x^2-y^2}$
13.0	$0.0132d_{z^2}$ $+0.09996d_{yz}$ $+0.0163d_{xz}$ $+0.0071d_{xy}$ $+0.0197d_{x^2-y^2}$
12.3	$0.0054d_{z^2}$ $-0.0154d_{yz}$ $+0.9986d_{xz}$ $+0.0014d_{xy}$ $-0.0513d_{x^2-y^2}$
0.0	$-0.0079d_{yz}$ $+0.9991d_{xy}$ $+0.0415d_{x^2-y^2}$

FIGURE 5 Comparison of the experimental (×) and calculated (——) e.s.r. data for $[MoOCl_3\{P(NMe_2)_3O\}_2]$ in (*a*) *ac**, (*b*) *bc**, (*c*) *ac* planes, and for tungsten-diluted $[NbOCl_3\{P(NMe_2)_3O\}_2]$ in (*d*) *ab*, (*e*) *bc** planes, and (*f*) the relative *d*-orbital energies and associated wave functions. The calculation was for the crystallographically determined geometry, e_σ (oxo) = 52.0 × 10^3, e_π (oxo) = 16.0 × 10^3, e_σ [Cl(2), Cl(3)] = 9.0 × 10^3, e_π [Cl(2), Cl(3)] = 1.9 × 10^3, e_σ [Cl(1), O(2)] = 12.0 × 10^3, e_π [Cl(1), O(2)] = 2.1 × 10^3, e_σ (OP_{trans}) = 5.0 × 10^3, e_π (OP_{trans}) = 0.0 cm^{-1}, k_x = 0.79, k_y = 0.81, k_z = 0.48, ξ_{Mo} = 695 cm^{-1}

$[MoOCl_3(PPh_3O)_2]$ *and* $[MoOCl_3\{P(NMe_2)_3O\}_2]$. The angular-overlap method has also been applied to the

e.s.r. data for these two compounds.[7,8] It is possible to obtain very good agreement between the observed and calculated data, two examples of which are shown in Figures 5 and 6. In the case of $[MoOCl_3\{P(NMe_2)_3O\}_2]$ the agreement between theory and experiment for the concentrated system is excellent (better than 0.1% in terms of magnetic fields at all orientations studied), but becomes slightly worse (maximum error *ca.* 0.5%) when the much better resolved data from the diluted system is considered. For $[MoOCl_3(PPh_3O)_2]$ the maximum error of *ca.* 0.6% in terms of magnetic field occurs in the *bc** plane.

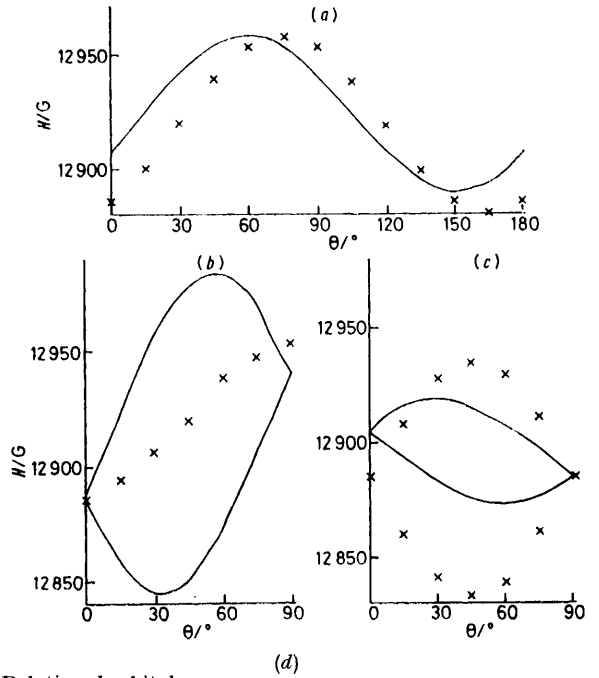

(*d*)

Relative *d*-orbital energies/10^3 cm^{-1}	Wave functions
59.6	$-0.9969d_{z^2}$ $-0.0112d_{yz}$ + $0.0059d_{xz}$ $+0.0183d_{xy}$ $+0.0754d_{x^2-y^2}$
22.8	$0.0751d_{z^2}$ $+0.0370d_{yz}$ $+0.0362d_{xz}$ $+0.0017d_{xy}$ $+0.9958d_{x^2-y^2}$
12.8	$-0.0046d_{z^2}$ $+0.5490d_{yz}$ $+0.8340d_{xz}$ $+0.0233d_{xy}$ $-0.0504d_{x^2-y^2}$
12.3	$-0.0131d_{z^2}$ $+0.8345d_{yz}$ $-0.5505d_{xz}$ $+0.0186d_{xy}$ $-0.0099d_{x^2-y^2}$
0.0	$0.0184d_{z^2}$ $-0.0282d_{yz}$ $-0.0094d_{xz}$ $+0.9994d_{xy}$ $-0.0018d_{x^2-y^2}$

FIGURE 6 Comparison of the experimental (×) and calculated (——) e.s.r. data for $[MoOCl_3(PPh_3O)_2]$ in (*a*) *ac**, (*b*) *ab*, (*c*) *bc** planes and (*d*) the relative *d*-orbital energies and associated wave functions. The calculation was for the crystallographically determined geometry, e_σ (oxo) = 52.0 × 10^3, e_π (oxo) = 16.0 × 10^3, e_σ [Cl(1), Cl(3)] = 12.0 × 10^3, e_π [Cl(1), Cl(3)] = 2.0 × 10^3, e_σ [Cl(2), O(2)] = 9.0 × 10^3, e_π [Cl(2), O(2)] = 1.8 × 10^3, e_σ (OP_{trans}) = 5.0 × 10^3, e_π (OP_{trans}) = 0.0 cm^{-1}, k_x = 0.70, k_y = 0.82, k_z = 0.52, and ζ_{Mo} = 695 cm^{-1}

In this communication we have been interested in exploring the feasibility of using the angular-overlap model for the interpretation of the e.s.r. data of low-symmetry second- and third-row transition-metal complexes. With this objective in mind we have not reported the detailed ranges of parameters that were examined. The investigations on $[MoOCl_3(PPh_3O)_2]$ and $[MoOCl_3\{P(NMe_2)_3O\}_2]$ suggest that the model may be as useful for the interpretation of the e.s.r. data on these molybdenum(v) complexes as it is for magnetic susceptibilities of first-row transition-metal complexes.[23] The method is currently being applied to other molybdenum(v) complexes in order to further test the model, and to determine whether or not the parameters used correlate with other physical and chemical properties of the systems. The application of the model to the single tungsten(v) complex has not been successful, although studies of compounds where the molecules are not disordered is desirable before this method of interpretation is rejected.

We thank the S.R.C. for support, and the Commonwealth Commission for the award of a Scholarship (to N. C. H.).

[9/1540 *Received*, 26*th September*, 1979]

REFERENCES

[1] C. D. Garner, M. R. Hyde, F. E. Mabbs, and V. I. Routledge, *J.C.S. Dalton*, 1975, 1175; 1180.
[2] C. D. Garner, M. R. Hyde, and F. E. Mabbs, *Nature*, 1975, **253**, 625.
[3] C. D. Garner, M. R. Hyde, F. E. Mabbs, and V. I. Routledge, *Nature*, 1974, **252**, 579.
[4] R. Durant, C. D. Garner, M. R. Hyde, F. E. Mabbs, J. R. Parsons, and D. Richens, *J. Less-Common Metals*, 1977, **54**, 459.
[5] C. D. Garner, L. Hill, N. C. Howlader, M. R. Hyde, R. E. Mabbs, and V. I. Routledge, *J. Less-Common Metals*, 1977, **54**, 27.
[6] C. D. Garner, L. H. Hill, D. L. McFadden, and A. T. McPhail, *J.C.S. Dalton*, 1977, 853; 1202.
[7] C. D. Garner, P. Lambert, F. E. Mabbs, and T. J. King, *J.C.S. Dalton*, 1977, 1191.
[8] C. D. Garner, N. C. Howlader, F. E. Mabbs, A. T. McPhail, and K. D. Onan, *J.C.S. Dalton*, 1978, 1848.
[9] B. A. Notton and E. J. Hewitt, *Biochem. Biophys. Res. Comm.*, 1971, **44**, 702.
[10] D. T. Cromer and J. T. Waber in ' International Tables for *X*-Ray Crystallography,' Kynoch Press, Birmingham, 1974, vol. 4, p. 101.
[11] D. T. Cromer and J. B. Mann, *Acta Cryst.*, 1968, **A24**, 321.
[12] R. F. Stewart, E. R. Davidson, and W. T. Simpson, *J. Chem. Phys.*, 1965, **42**, 3175.
[13] D. T. Cromer and D. Liberman, *J. Chem. Phys.*, 1970, **53**, 1891.
[14] SHELX-76, Crystallographic Calculation Program, G. M. Sheldrick, University of Cambridge.
[15] PLUTO, Program for Crystallographic Drawing, W. D. Motherwell, University of Cambridge.
[16] C. D. Garner, P. Lambert, F. E. Mabbs, and J. K. Porter, *J.C.S. Dalton*, 1972, 30.
[17] D. L. McFadden, A. T. McPhail, C. D. Garner, and F. E. Mabbs, *J.C.S. Dalton*, 1975, 263.
[18] A. T. McPhail, personal communication.
[19] D. S. Schonland, *Proc. Phys. Soc.*, 1959, **73**, 788.
[20] C. D. Garner, N. C. Howlader, F. E. Mabbs, P. M. Boorman, and T. J. King, *J.C.S. Dalton*, 1978, 1350.
[21] M. Gerloch and R. C. Slade, ' Ligand Field Parameters,' Cambridge University Press, 1973.
[22] A. Abragam and M. H. L. Pryce, *Proc. Roy. Soc.*, 1951, **A205**, 135.
[23] D. A. Cruse and M. Gerloch, *J.C.S. Dalton*, 1977, 152; 1613; 1617; M. Gerloch and I. Morgenstern-Badarau, *ibid.*, 1619.